

PID Control Assessment Using L-Moment Ratio Diagrams

Paweł D. Domański ^{1,*}, Krzysztof Dziuba ² and Radosław Góra ²

¹ Institute of Control and Computation Engineering, Faculty of Electronics and Information Technology, Warsaw University of Technology, Nowowiejska 15/19, 00-665 Warsaw, Poland

² Grupa Azoty Zakłady Azotowe "PUŁAWY" S.A., al. Tysiąclecia Państwa Polskiego 13, 24-110 Puławy, Poland; krzysztof.dziuba@grupazoty.com (K.D.); radoslaw.gora@grupazoty.com (R.G.)

* Correspondence: pawel.domanski@pw.edu.pl

Abstract: This paper presents an application of L-moments and respective L-moment ratio diagrams (LMRD) to the task of control performance assessment (CPA). An L-moment ratio diagram is a graphical approach to the visualization of statistical properties for a given time series. Moreover, it enables comparing various data, showing their similarities and homogeneity. Simultaneously, CPA aims at measuring the control loop quality, supporting decision-making about their tuning and maintenance. This paper shows that control system quality can be efficiently visualized using LMRDs. The method was analyzed using simulations and further validated at a real chemical engineering industrial ammonia synthesis plant.

Keywords: control performance assessment; moment ratio diagrams; L-moments; PID; power generation

1. Introduction

The task of a control engineer is to design, tune, and maintain control systems, which allow a given installation to work according to the assumed requirements. To fulfill these activities, one must have enough skills, knowledge about the process, and updated information about the actual performance of the control system. Control performance assessment tasks support an engineer with information about how the control system operates [1]. Thus, CPA plays a very important role in maintaining the control system and the desired performance of the operation of the actual plant. When the control system does not fulfill its requirements, the whole installation also misses its targets and performs inconsistently with expectations [2].

Despite the fact that this knowledge has been well known for decades, it is still the case that industrial systems often do not operate as demanded [3–5], which is caused by process difficulties (non-stationarity, disturbances and noises), hardware problems (actuators, sensors, IT infrastructure), human errors or inattention (inadequate maintenance, design or tuning), or just a general lack of time or proper knowledge [6,7].

The key performance indicators (KPIs) depend on the type of plant, engineering culture, and tradition; however, no matter what these are, CPA activities and measures have to be applied using a reliable and transparent approach. In process industry, the proportional-integral-derivative (PID) algorithm constitutes the backbone of control strategies. It is used in an overwhelming majority, i.e., more than 90% or even 95% of industrial control loops [8–10].

The story started in 1967 with a pulp and paper plant and its performance assessment using variable standard deviation [11]. Since then, the method has evolved dramatically, exploring and exploiting various research areas and approaches [12]. Nowadays, investigations address numerous methods [13], like the ones that require plant parametric experiments [14], which use process model identification [15,16], or that model-free techniques that need plant data only [17,18]. Apart from homogeneous approaches,



Citation: Domański, P.D.; Dziuba, K.; Góra, R. PID Control Assessment Using L-Moment Ratio Diagrams. *Appl. Sci.* **2024**, *14*, 3331. <https://doi.org/10.3390/app14083331>

Academic Editor: Yutaka Ishibashi

Received: 2 April 2024

Revised: 10 April 2024

Accepted: 12 April 2024

Published: 15 April 2024



Copyright: © 2024 by the authors. Licensee MDPI, Basel, Switzerland. This article is an open access article distributed under the terms and conditions of the Creative Commons Attribution (CC BY) license (<https://creativecommons.org/licenses/by/4.0/>).

there are proposals to use hybrid techniques that use the fusion of various measures and approaches [19,20].

As a result, we do not end up with a single and universal approach. There is a large spectrum of methods, and an engineer is generally lost, as he has to select an appropriate method. As a result, we demand hybrid and multi-criteria approaches that allow supporting control loop performance decision-making. In this task, statistical methods, which have been a bit forgotten but are still characterized by enduring advantages, can come to our rescue. Moment ratio diagrams (MRD) deliver such a tool [21], which have actually been known in statistics for decades [22] as MRDs originated from Pearson's research in the early 19th century. Moment ratio diagrams graphically compare different statistics of a given time series to visualize properties of the stochastic process, which is hidden behind data. A MRD can be used in various tasks, such as fitting of empirical data to theoretical probabilistic density functions (PDFs), comparison of the PDF shapes, and the classification of data [23]. A MRD is a two-dimensional graphical diagram in a Cartesian coordinate system for a pair of selected statistical moments.

As L-moments constitute a robust version of the common definition of statistical moments [24], an L-moment ratio diagram (LRMD) exploits and extends the idea of the MRD. LMRD plots are extensively used in life sciences, like seismology [25], hydrology [26], astronomy [27], meteorology [28], medicine [29], and many others [30]. Their utilization in engineering sciences and specifically in control technology is extremely rare. This paper fills this observed research gap.

Any research that addresses aspects of control performance validation, their design, or tuning remains unsatisfactory if it is limited to theoretical or simulation considerations only. Only industrial verification of theoretical ideas tested by simulation makes it possible to definitively confirm their sense and practical applicability. Simulation studies make it possible to safely and quickly verify various ideas, before their plant tests, which bring ultimate confirmation. Such an arrangement of activities is presented in this paper. Simulation studies for classical benchmarks for PID controllers preceded industrial validation conducted at an ammonia plant at Grupa Azoty, Zakłady Azotowe "Puławy" SA in Poland. The industrial validation used long-term data from the plant's operation collected after a project of comprehensive modernization of the installation control system, i.e., the design, tuning, and implementation of an advanced process control (APC) solution.

The main contribution of this work is the introduction of an LMRD to control the performance assessment. This work consists of two elements. First, a simulation analysis was performed using common process PID control benchmarks. Next, an industrial validation was performed using an ammonia synthesis installation. Different from standard LMRD formulations, a new and appropriate scheme of LMRD is proposed and tested. The research compared the applied L-moments using well-known control performance measures: integral square error (ISE), integral absolute error (IAE), and basic KPIs of the control loop step response: overshoot (κ) and settling time (T_{set}). Finally, the LMRDs were validated in a real application from the heat power generation industry. This paper starts with Section 2 describing the methods followed by the simulation analysis included in Section 3. Section 4 presents the industrial study results and Section 5 concludes the work and presents observed open issues for further research.

2. Applied methods

The work uses selected statistical and control performance assessment methods, which are described below: basic integral control error measures, and statistical moments and L-moments, which are utilized in the proposed LRMD.

2.1. CPA Integral Indexes

The main integral indexes used for control loop assessment are the integral square error and integral absolute error. They are evaluated using a selected norm for the control error signal, which is the difference between the setpoint (STP) and process variable (PV),

often also denoted as a CV—controlled variable. The ISE we evaluate is the mean integral of the squared control errors $\epsilon(k)$ (norm ℓ_2)

$$\text{ISE} = \frac{1}{N} \sum_{k=1}^N \epsilon^2(k). \quad (1)$$

In practical implementations, we exchange an integral with the summation of control errors collected in sampled time moments $k = 1, \dots, N$. Integral square measure penalizes those errors, which exhibit large values, neglecting the ones with small values. As large control errors frequently occur as a result of large disturbances or rapid setpoint changes, the ISE favors control aggressiveness and disregards small but continuing imbalances like oscillations. Statistically, the ISE measure is seriously affected by outlying observations and exhibits a 0% breakdown point [31].

The IAE index sums the errors' absolute values over a given time period, i.e., it uses the ℓ_1 norm of the control error

$$\text{IAE} = \frac{1}{N} \sum_{k=1}^N |\epsilon(k)|. \quad (2)$$

This measure is much less conservative than ISE, and it allows penalizing continuing oscillations, which are comparable to large error incidents. Although the breakdown point of IAE also equals 0%, it is shown that this measure exhibits robustness against some kinds of outliers, i.e., the outliers in OX. This is much more important in the case of time series, as those anomalies reflect outlying time observations.

2.2. Statistical Moments

We may utilize statistics in many different ways. We often calculate the data mean or standard deviation for some empirical data to show basic properties, i.e., its expected value and fluctuations. We may also address the problem in a different way using a theoretical approach. We fit an appropriate distribution model, a PDF function, to the data and then use its factors or moments (if they exist) to characterize the data.

In this approach, we use an empirical approach and consider appropriate estimators for basic statistical moments. Let us assume that $\{X_i\}^T$ denotes a given time series with its expected value, mean μ (the first statistical moment) and the r th central moment $\gamma_r = E(X - \mu)^r$, where $E(\cdot)$ represents the expectation operator. The mean μ denotes the first moment γ_1 , while variance σ^2 represents the second moment denoted as γ_2 , where σ indicates standard deviation.

The first two moments are frequently supplemented in analyzes by the third γ_3 moment called skewness and the fourth γ_4 —the kurtosis. The data skewness factor reflects its asymmetry, with its value equal to zero for symmetrically distributed data. Kurtosis relates to the data concentration

$$\gamma_3 = \frac{1}{N\sigma^3} \sum_{i=1}^N (x_i - \mu)^3, \quad (3)$$

$$\gamma_4 = \frac{1}{N\sigma^4} \sum_{i=1}^N (x_i - \mu)^4 - 3. \quad (4)$$

The above estimators can be used to evaluate the first four moments for a given empirical time series. The existence of data contamination in the form of outlying observations (those originating from different stochastic process) in data biases statistical analyzes and estimations. Outliers change the shape of a distribution function, increasing or extending its tails. They cause heavy or long tails in PDFs [32].

This feature biases classical estimators of statistical moments, making them inappropriate. This fact causes artificially increased values of the standard deviation and biased

mean. To cope with this problem, we may use its robust counterparts like the median for the expected value, mean absolute deviation (MAD) for variance, trimmed estimators, and many others [33]. The other approach is to use L-moments, which are also robust against outliers and simultaneously introduce other advantages into the analyses.

2.3. L-Moments

Hosking [24] proposed the notion of L-moments as a linear combination of ordered statistics. This theory incorporates a new description of the distribution function shape, supports the task of the estimation of coefficients for an assumed PDF and enables testing hypotheses about eventual theoretical distributions. We define the L-moments for any random variable, for which the moments exist. The L-moments allow obtaining an almost unbiased estimation, even for a very small observation sample. Additionally, the L-moment estimators are robust against outliers and the distribution function tails [34]. The above properties are highly appreciated in the life sciences. However, the same observation might be made in the engineering sciences, and control is not an exception.

We evaluate L-moments according to the following algorithm. At first, the data $\{x_1, \dots, x_N\}$, N —number of samples, are ranked in ascending order from 1 to N . In the consecutive step, the sample L-moments (l_1, \dots, l_4) are evaluated, followed by the sample L-skewness τ_3 and L-kurtosis τ_4 . The algorithm equations are sketched below:

$$\begin{aligned} l_1 &= \beta_0, \quad l_2 = 2\beta_1 - \beta_0, \\ l_3 &= 6\beta_2 - 6\beta_1 + \beta_0, \\ l_4 &= 20\beta_3 - 30\beta_2 + 12\beta_1 - \beta_0, \\ \tau_2 &= \frac{l_2}{l_1}, \quad \tau_3 = \frac{l_3}{l_2}, \quad \tau_4 = \frac{l_4}{l_2}, \end{aligned} \tag{5}$$

where

$$\beta_j = \frac{1}{N} \sum_{i=j+1}^N x_i \frac{(i-1)(i-2) \cdots (i-j)}{(N-1)(N-2) \cdots (N-j)}. \tag{6}$$

These formulation of moments allow obtaining the shift estimator, i.e., the L-shift l_1 , two scaling factors in the form of the L-scale $l_2 \in [0, 1)$, L-covariance denoted as L-Cv $\tau_2 > 0$, and two higher moments: L-skewness $\tau_3 \in (-1, 1)$ and L-kurtosis $\tau_4 \in \left(-\frac{1}{4}, 1\right)$.

L-moments can be applied to many tasks; for instance, in the modified method-of-moments for theoretical distribution fitting to empirical data. L-skewness and L-kurtosis are used as a proper goodness-of-fit measure. We can evaluate L-moments for theoretical distribution functions as well [35]. As an example, the L-moments for a normal distribution are as follows: $l_1 = \mu$, $l_2 = \frac{\sigma}{\pi}$, $\tau_3 = \frac{l_3}{l_2} = 0$ and $\tau_4 = \frac{l_4}{l_2} = 0.1226$.

It should be noted that L-moments have allowed the introduction of several other ordered-type estimators such as trimmed TL-moments [36], LL- [37], LH- [38], LQ- [39], and PL- moments [40].

2.4. Moment Ratio Diagrams

Moment ratio diagrams graphically present empirical or theoretical statistical properties of given data in a two-dimensional plane. Practically, we use two versions of MRD diagrams [41]. A MRD(γ_3, γ_4) presents the relationship between the third γ_3 moment (or its square γ_3^2 in some realizations) plotted as the abscissa and the fourth one, γ_4 drawn as the ordinate. The kurtosis is often drawn upside down. One should remember that there is a theoretical constraint on the accessible area on a diagram, due to the following relationship:

$$\gamma_4 - \gamma_3^2 - 1 \geq 0. \tag{7}$$

Each distribution function can be represented by a point, curve, or region. This representation depends on the number of PDF shape parameters. Distribution functions

that do not have shape factors (like Gauss, Laplace, or Cauchy) are reflected by a single point. The functions that have one shape factor, like the generalized extreme value (GEV), are drawn as a curve. Regions reflect distributions parameterized by two shape factors, like the α -stable distribution of four parameter kappa (K4P). The second type of diagram, i.e., the MRD(γ_2, γ_3), relates the variance γ_2 drawn as the abscissa with the skewness γ_3 at the ordinate. However, this diagram is location- and scale-dependent, which makes it less useful.

2.5. L-Moment Ratio Diagrams

The notion of L-moments was introduced by Hosking [24]. As L-moments extend the background idea of moments, it was natural to introduce the LMRD as an extension of the idea of MRDs. The LMRD is a popular tool in extreme value analysis (EVA). They allow identifying the proper distribution for empirical observations. The plot that relates L-kurtosis τ_4 to L-skewness τ_3 denoted as LMRD(τ_3, τ_4) is the most common variant. By analogy to MRDs, we may compare any empirical data against various theoretical distribution functions [34].

Similarly to MRDs (γ_2, γ_3), there are two LMRD variants and the LMRD(τ_2, τ_3) is also used. This research suggests also using the third type of diagram, i.e., the LMRD(l_2, τ_4). It is shown that its properties are more useful in the control engineering context.

The idea behind using LMRDs rests on the fact that there exists an assumption that properly controlled variables should meet Gaussian properties. This means that the process is linear, symmetric, stationary, all the disturbances are properly decouples, and there are no extraordinary human interventions, like manual control mode. In such a case, one expects that the associated points on the LMRD(τ_3, τ_4) diagram will be close to the point (0, 0.1226), and in LMRD(τ_2, τ_3), this is as close as possible to the origin (0, 0) and $\tau_3 \approx 0$.

3. Simulation Research

A dedicated Matlab simulation layout was designed to analyze the single element PID control loop. It is sketched in Figure 1. We used a parallel form of the PID algorithm defined as

$$G_{PID}(s) = k_p(1 + \frac{1}{T_i s} + T_d s). \tag{8}$$

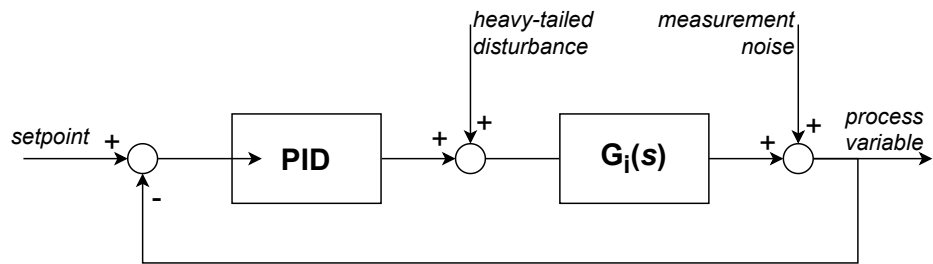


Figure 1. The simulation close-loop system diagram.

To assess the effectiveness of the LMRD diagrams, we simulated three univariate PID controls with three plants, which were proposed by Åström [42] as control benchmarks:

- multiple equal pole transfer function,

$$G_1(s) = \frac{1}{(s + 1)^4}, \tag{9}$$

- first-order transfer function with a dead time,

$$G_4(s) = \frac{1}{(0.2s + 1)^2} e^{-s}, \tag{10}$$

- fast and slow mode transfer function,

$$G_5(s) = \frac{1}{(s+1)(0.04s^2 + 0.04s + 1)}. \quad (11)$$

Such a selection allowed running the analysis taking into account a wide spectrum of possible processes, which can be met in process industry. The simulation loops were sampled with a time period of $\Delta T = 0.1$ s. The setpoint signal was set to a constant zero value. Moreover, two disturbances were introduced into the loops. They simulated potential industry-like effects:

- the Gaussian $N(0, \sigma^2)$ measurement noise with standard deviation $\sigma = 0.1 \cdot \sqrt{2}$, which was added at the plant output to the process variable;
- filtered heavy-tailed disturbance, which was added before the plant transfer function, and which was simulated as a SaS stochastic process based on the α -stable distribution random number generator with the stability exponent $\alpha = 1.95$ and scaling factor $\gamma = 2.0$ [43].

All PID controllers were tuned using performance index optimization, according to three weighted criteria: the integral of time-weighted absolute error (ITAE) criterion (weight $w_1 = 1$), maximum overshoot ($w_2 = 10$), and sensitivity ($w_3 = 20$), as proposed in [44]. These settings are referred to hereafter as well-tuned and are shown in Table 1.

Table 1. Parameters for the well-tuned PID controllers.

	k_p	T_i	T_d
$G_1(s)$	1.0503	2.9977	0.9293
$G_4(s)$	0.2653	0.6066	0.2121
$G_5(s)$	0.1330	0.2585	0.0808

A detailed analysis with the whole set of considered diagrams is presented for the first transfer function $G_1(s)$, while the other two processes are assessed by selecting the most promising diagram, i.e., the LMRD(l_2, τ_4). Figure 2 shows the sample control error time series for the $G_1(s)$ transfer function controlled by the so called well-tuned controller, with its parameters as in Table 1.

The analysis assessed and compared various settings of the PID algorithm. The gain $k_p \in [0.05; 2.05]$ was changed every 0.25 step, the integration time $T_i \in [0.2; 10.2]$ was changed every 1.0, while the derivative time constant was set to a constant $T_d = 0.9293$. Altogether, we used further comparison results for 99 various control loops. To exclude statistical effects, each set of parameters was run 50 times and the evaluated L-moment values were averaged. We related the obtained controller performance to common and well-understood loop quality indexes. We used overshoot, settling time, ISE, and IAE for that purpose. This relationship was included in all LMRDs in the form of the respective shading of the circles representing each tuning.

Figure 3 shows the respective LMRDs(τ_3, τ_4) related to the overshoot. We can observe that, generally, the majority of loops exhibited a low overshoot. Those few that had significant value of overshoot were characterized by an increased L-kurtosis τ_4 compared to the normal distribution and $\tau_4 = 0.1226$. We may also observe that the scatter of points with respect to the OX axis denoting skewness τ_3 was small and insignificant within a narrow set of $\tau_3 \in (-0.01, 0.01)$.

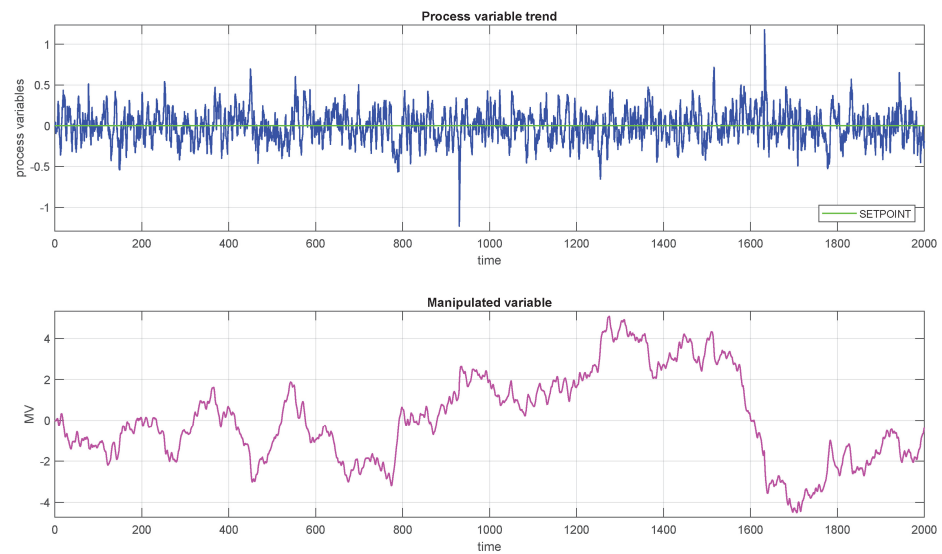


Figure 2. Time series for the loop $G_1(s)$, which was run using the so-called well-tuned PID algorithm (blue line—process variable, green—setpoint, magenta—manipulated variable).

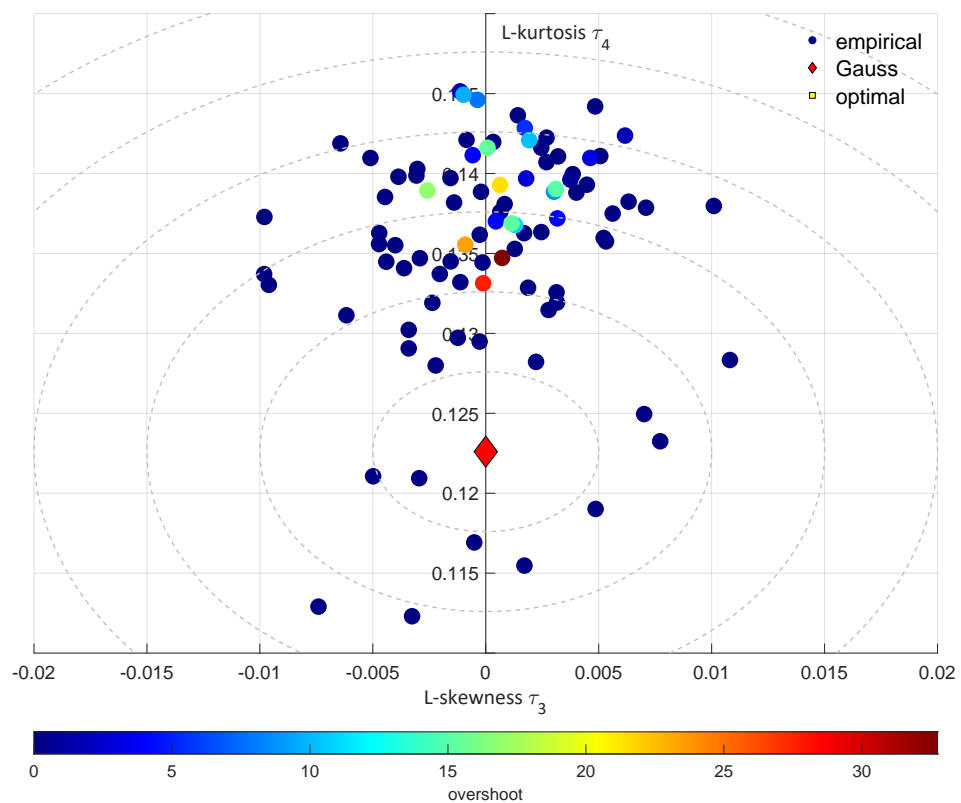


Figure 3. The LMRD(τ_3, τ_4) for $G_1(s)$ related to overshoot κ .

Following the above presentation scheme, Figure 4 shows the analogous relationship related to the settling time T_{set} . We see quite a contrary behavior, as the loops that exhibited a long settling time are represented by points with a lower L-kurtosis value.

Generally, these two plots confirm the contradictory meaning of the overshoot and the settling time. Higher accuracy was achieved at the cost of the settling time, and conversely speeding up the control led to a lower accuracy and introduced oscillations represented by the overshoot.

The next two diagrams extend the analysis, as they introduce the integral indexes. Figure 5 shows how the varying ISE index (norm ℓ_2) is represented in the $\text{LMRD}(\tau_3, \tau_4)$, while Figure 6 presents the effect of the norm ℓ_1 .

We can observe that both integrals ISE and IAE reacted similarly to the settling time, while the direct difference between ISE and IAE was less significant. We can only observe that IAE made a bit more of a mutual distinction between control loops, while ISE was, one might say, more binary in making a sharper distinction. This separation between the norms ℓ_2 and ℓ_1 is visible. This observation confirms that the meaning of the ISE and IAE is significant and should be considered in the selection of a performance index.

Additionally, the $\text{LMRD}(\tau_3, \tau_4)$ diagram is characterized by one shortcoming, as it has no possibility of reflecting loop fluctuations, which is naturally addressed by scale factors, like L-scale ℓ_2 or L-Cv τ_2 .

One may assume that similar observations of the overshoot and three other indexes might also appear for the other plots. As the same effect was observed, the following analysis is presented in the form of two types of diagrams related to the overshoot and settling time. Figures 7 and 8 present respective $\text{LMRDs}(\tau_2, \tau_3)$. The incorporation of the scale factor L-Cv τ_2 into the assessment enabled showing an appropriate separation between the poor and worse tunings in all cases. Additionally, the contradictory meaning for κ and T_{set} remained.

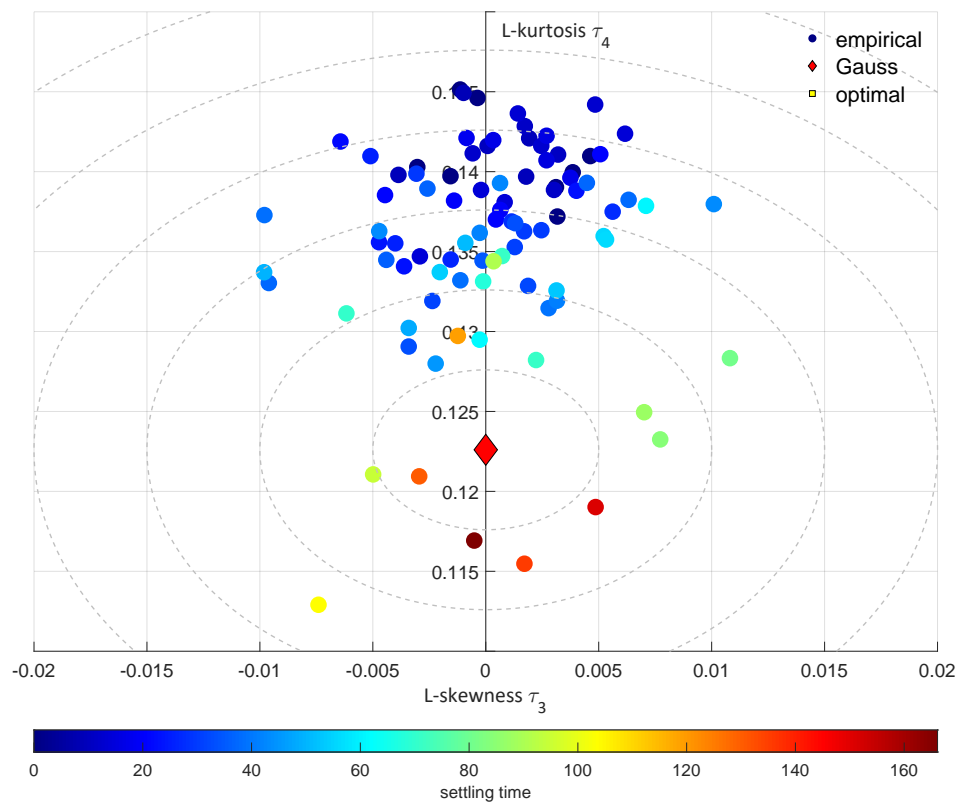


Figure 4. The $\text{LMRD}(\tau_3, \tau_4)$ for $G_1(s)$ related to settling time.

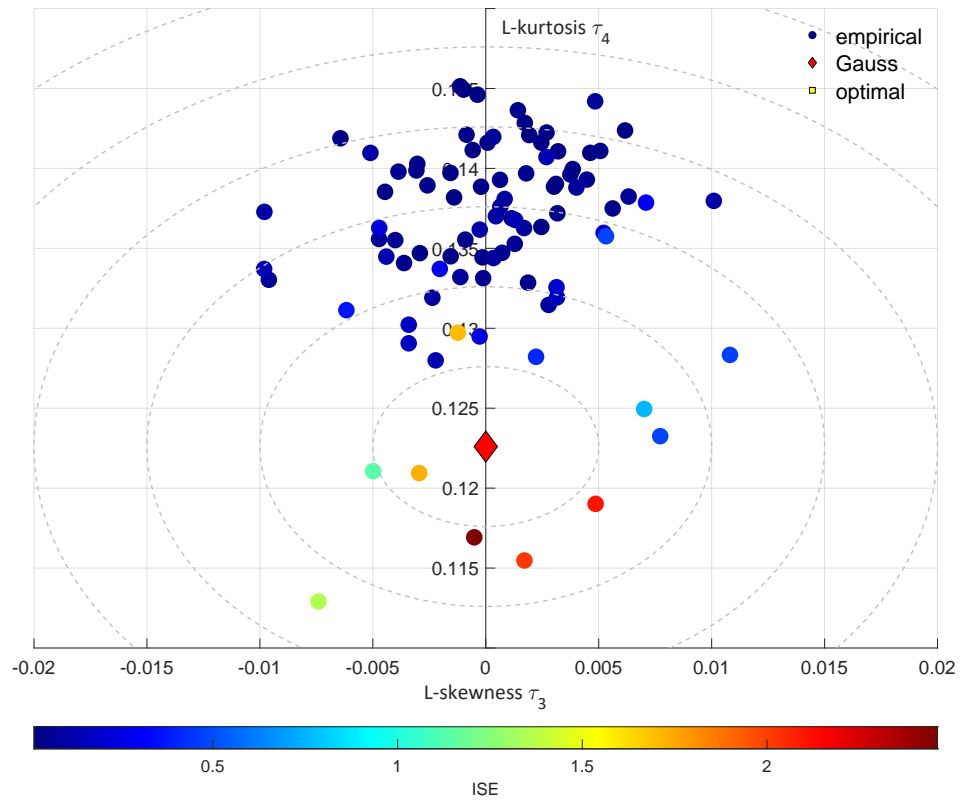


Figure 5. The LMRD(τ_3, τ_4) for $G_1(s)$ related to ISE.

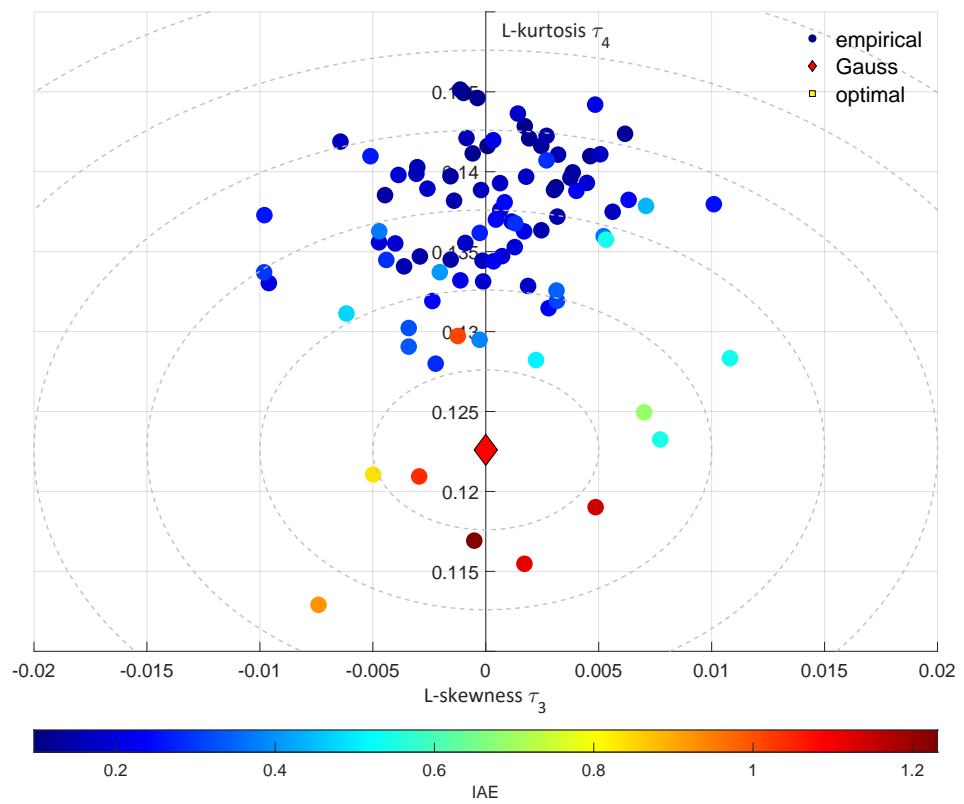


Figure 6. The LMRD(τ_3, τ_4) for $G_1(s)$ related to IAE.

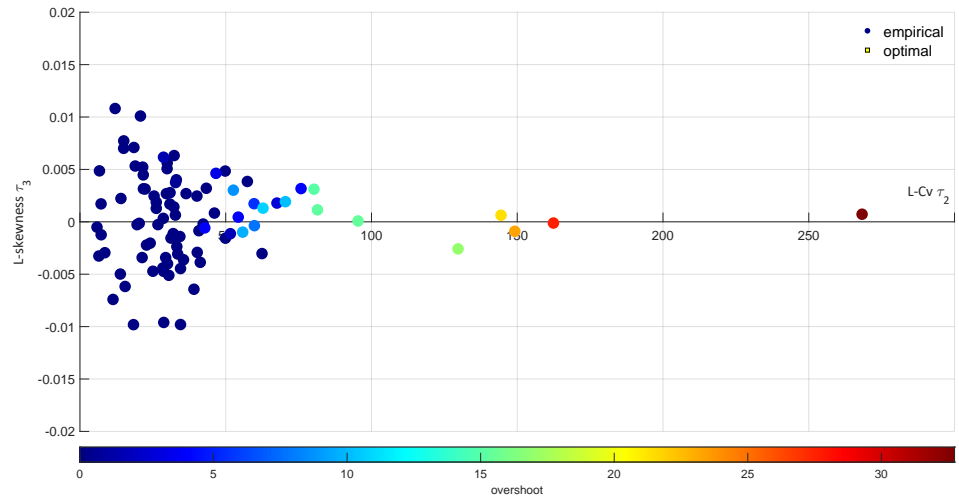


Figure 7. The LMRD(τ_2, τ_3) for $G_1(s)$ related to overshoot.

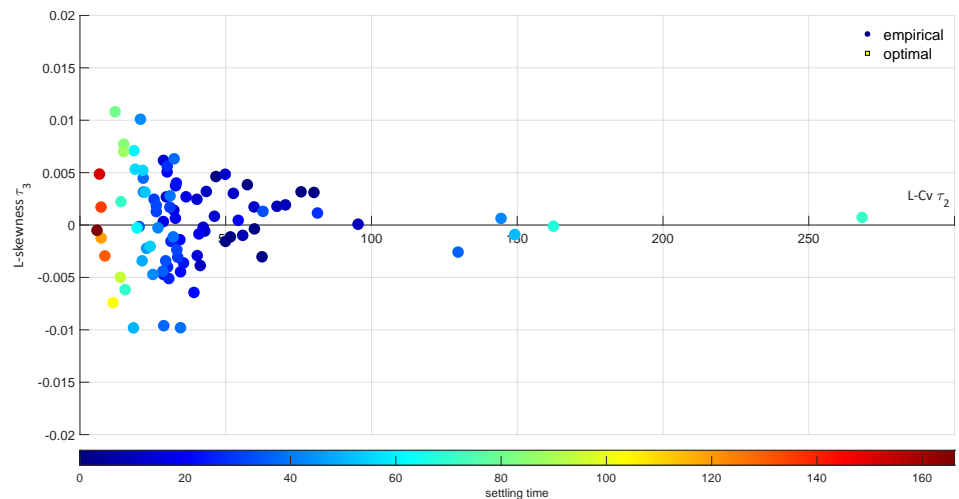


Figure 8. The LMRD(τ_2, τ_3) for $G_1(s)$ related to settling time.

Unfortunately, for the LMRDs(τ_2, τ_3), we observed that the L-Cv τ_2 value was not limited, and the OX axis scaling depended on data values. The use of the scaled l_2 moment should have addressed this issue. Figures 9 and 10 show LMRDs(l_2, τ_3) related to the overshoot and settling time. Unfortunately, we did not obtain a full improvement. The plots were scaled according to the known limits, but the separation related to the overshoot was lost. In such a case, there is no way to determine between high and low κ values using the LMRD(l_2, τ_3). This meant that the control performance could not be fully assessed using the LMRD(l_2, τ_3).

Finally, we introduced a new type of LMRD that compares L-kurtosis with L-moment l_2 . Figures 11 and 12 show the LMRD(l_2, τ_4) plots related to the overshoot and settling time.

We still observed a good separation for the settling time, while high overshoot performance detection was hard to accomplish. We may conclude that any single LMRD does not allow solving the assessment issue. There are two reasons for this: the overshoot detectability, and there being three statistical factors related to the control performance: scale, skewness, and kurtosis. Therefore, it is suggested to use a combination of two plots: the LMRD(τ_2, τ_3) and the LMRD(l_2, τ_4) or LMRD(τ_3, τ_4).

Further simulation analysis was conducted for two other transfer functions: $G_4(s)$ and $G_5(s)$. The way the simulations were run was similar to the $G_1(s)$ plant. For the $G_4(s)$ transfer function, the $k_p \in \langle 0.2; 1.6 \rangle$ changed its value every 0.2, the integration time $T_i \in \langle 0.1; 5.1 \rangle$ changed every 0.5, and the derivative time was kept constant at $T_d = 0.2121$. Thus, we obtained 88 points for the assessment analysis. For the $G_5(s)$ transfer function,

the $k_p \in \langle 0.02; 1.02 \rangle$ changed every 0.1, the integration time $T_i \in \langle 0.05; 2.3 \rangle$ changed every 0.25, and the derivative time $T_d = 0.0808$. Thus, we obtained 110 points for the assessment analysis of the $G_5(s)$ plant.

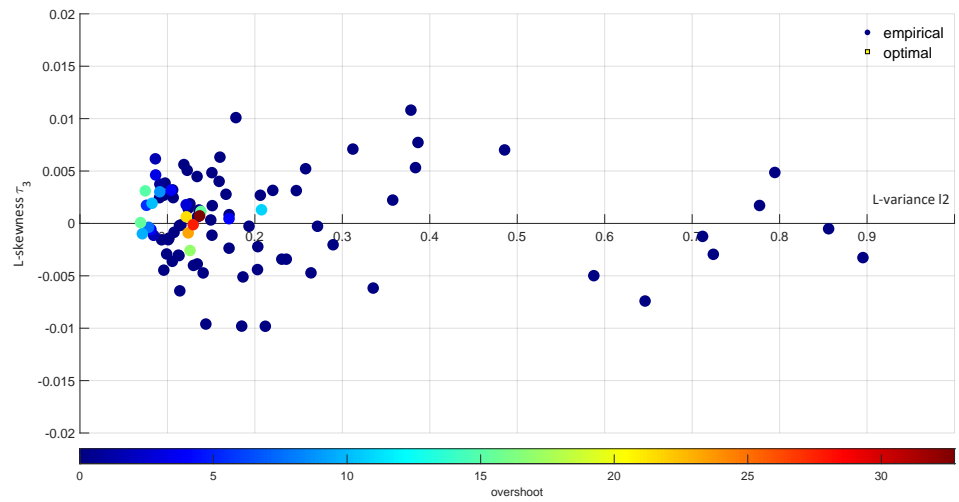


Figure 9. The LMRD(l_2, τ_3) for $G_1(s)$ related to overshoot.

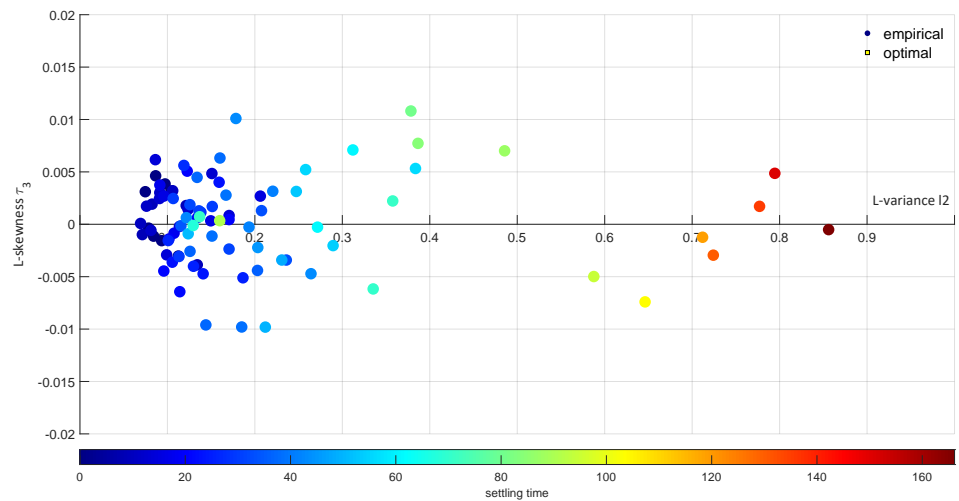


Figure 10. The LMRD(l_2, τ_3) for $G_1(s)$ related to settling time.

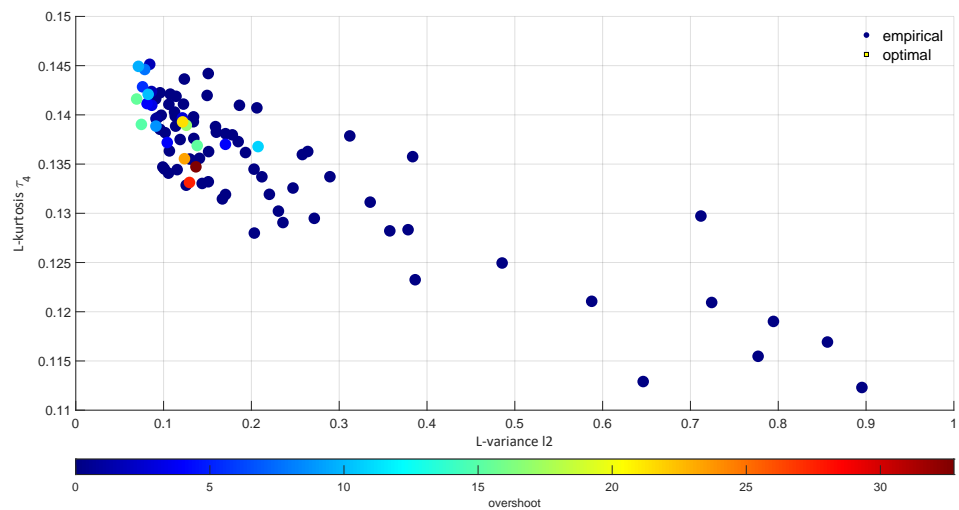


Figure 11. The LMRD(l_2, τ_4) for $G_1(s)$ related to overshoot.

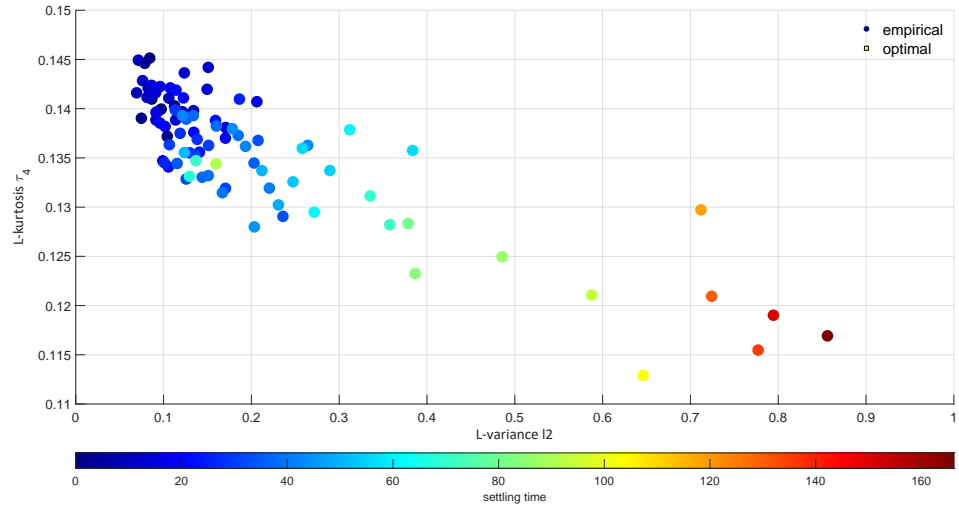


Figure 12. The LMRD(l_2, τ_4) for $G_1(s)$ related to settling time.

In order to protect this document from being overloaded with an unnecessary amount of charts, each process is only assessed with three plots, only allowing the two above combinations of diagrams with their relationship to one selected known index. Figures 13–15 show diagrams allowing the assessment of the $G_4(s)$ process.

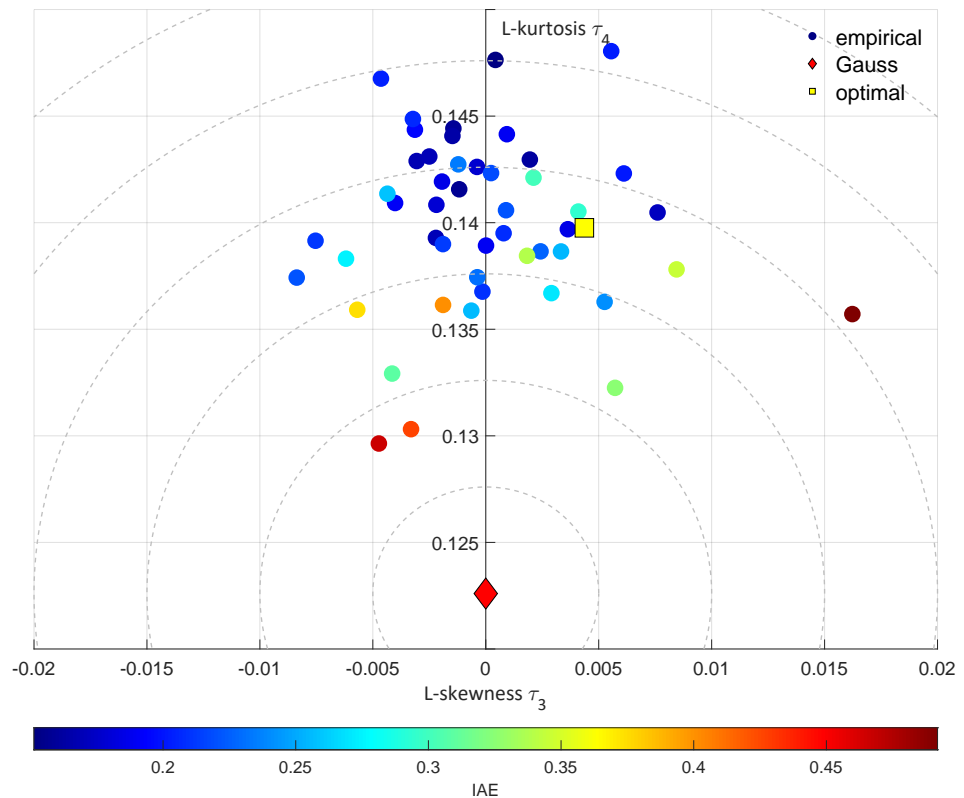


Figure 13. The LMRD(τ_3, τ_4) for $G_4(s)$ related to IAE.

The first combination of the LMRD(τ_2, τ_3) and the LMRD(l_2, τ_4) allows a relatively good detectability, while the second one might be somehow unclear, due to the properties of the LMRD(τ_3, τ_4) plot. These plots show the optimal well-tuned parameter set (the yellow square). It was close to the similar tuning, and the poor ones were distant from it.

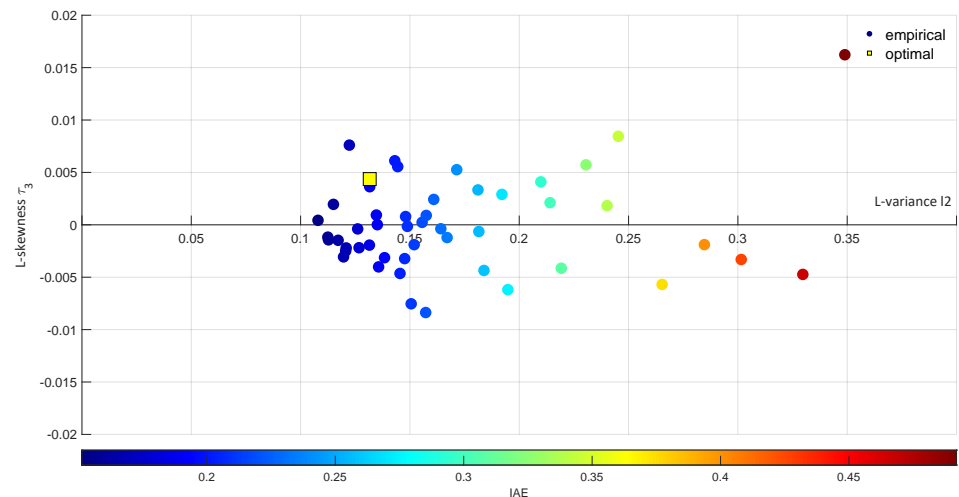


Figure 14. The LMRD(l_2, τ_3) for $G_4(s)$ related to overshoot.

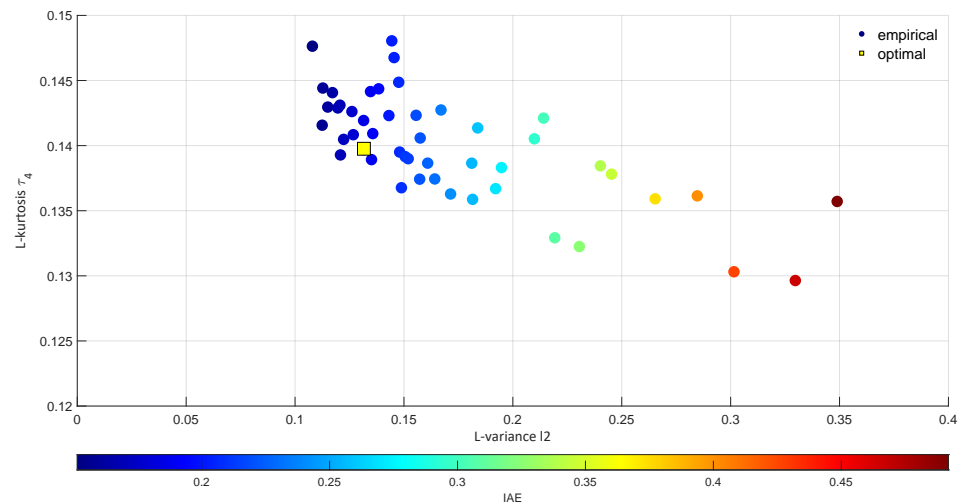


Figure 15. The LMRD(l_2, τ_4) for $G_4(s)$ related to overshoot.

Figures 16–18 show the analogous analysis for the $G_5(s)$ transfer function. These plots show the relation to the overshoot. In this case, we may observe that the scale factor l_2 allowed detecting a high overshoot. This observation points out that this issue requires further investigations.

It must be noted that the simulation experiments were designed in such a way so as to not introduce any unneeded asymmetrical effects into the data. This was done intentionally, as we did not want to introduce another degree of freedom into the analysis. Generally, such asymmetric properties might be introduced by operating point changes, i.e., changes in the setpoint or by process nonlinearities, such as actuator saturation or a wrong definition of the operating point close to the process technological constraints. These effects are not directly associated with the loop tuning. Setpoint fluctuations originate from the plant operation requirements, and actuator saturation is caused by the actuating element, while operation close to the constraints is the result of an inappropriate design or external production demands, such as a need to work with an over- or under-loaded production.

The simulation analysis enabled changing the controller tuning as we wished, and we did not have to worry about poor system performance, which might cause economic losses in the installation operation or might even cause instabilities. In real situations, we do not have such comfort and we only have a single controller tuning set (or maybe only a few, which have been used during the controller tuning procedure). Therefore, an assessment with a LMRD plot becomes tougher, as we need to perform an assessment using one point.

Its placement in the diagram depends on the control performance on the one hand, but is also affected by the process behavior. Thus, we cannot definitely say that any obtained position in the LMRD point is better or worse and what is the cause: the controller or the plant. An analogous conclusion follows from the use of IAE or ISE. Any single value of the integral index has no practical meaning.

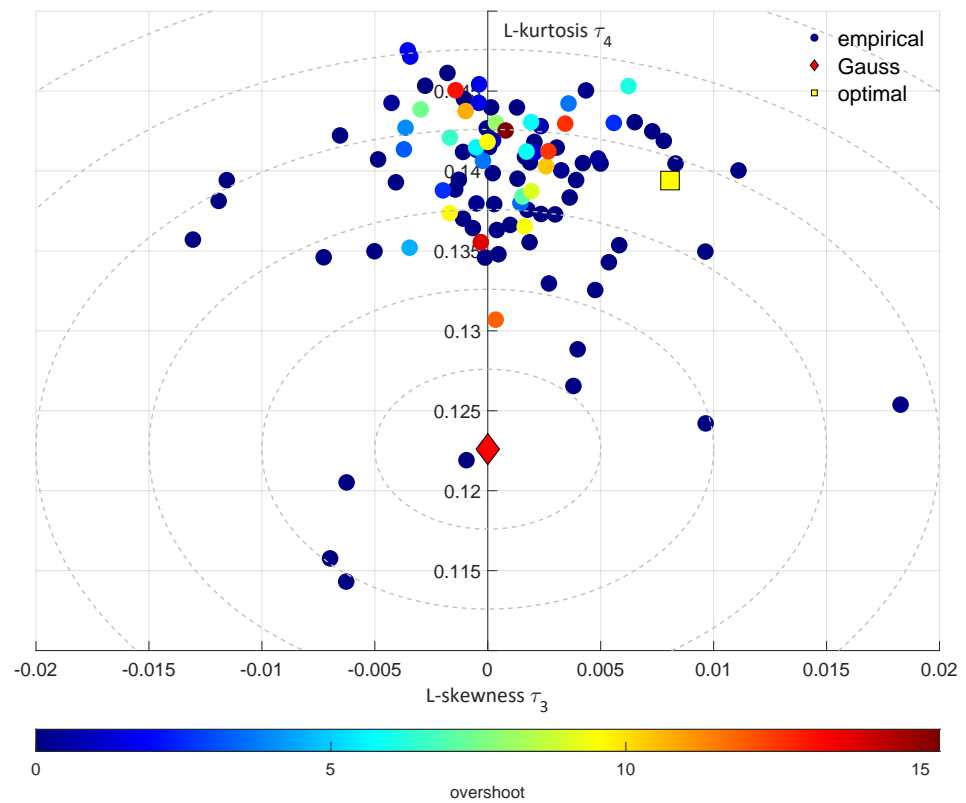


Figure 16. The LMRD(τ_3, τ_4) for $G_5(s)$ related to IAE.

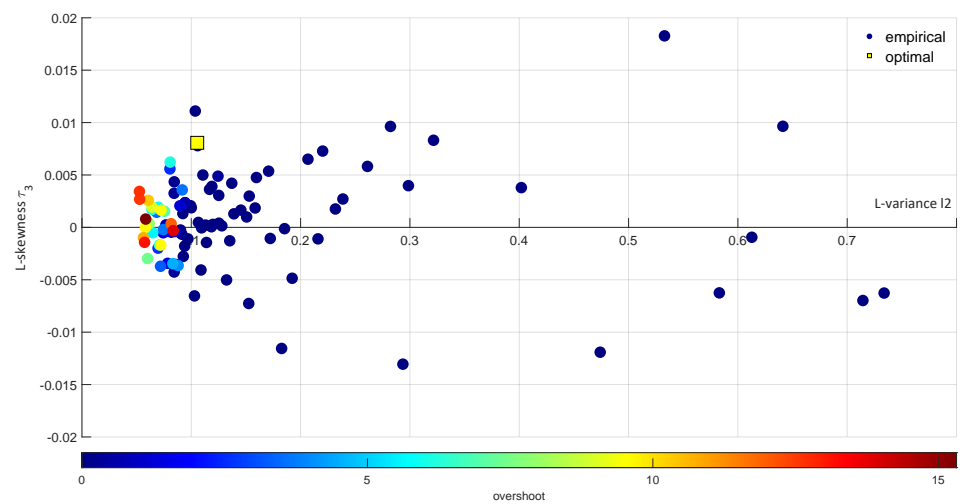


Figure 17. The LMRD(l_2, τ_3) for $G_5(s)$ related to overshoot.

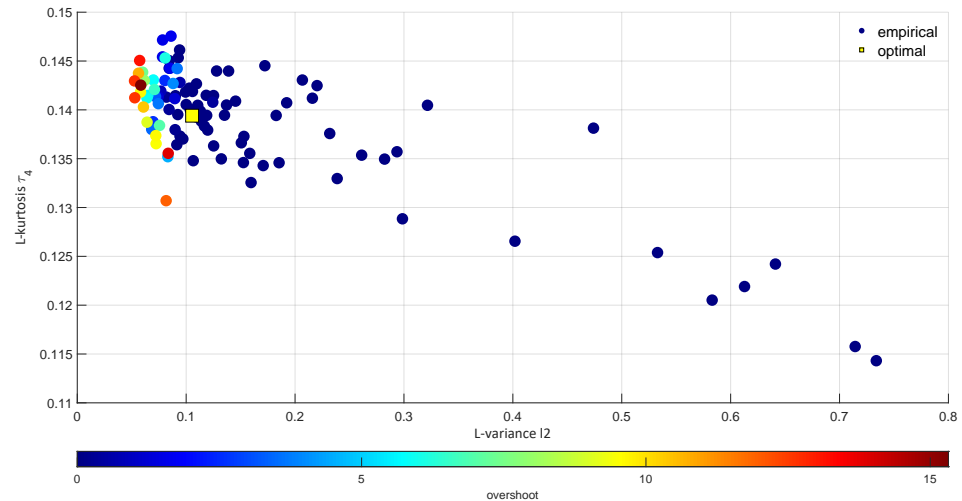


Figure 18. The LMRD(l_2, τ_4) for $G_5(s)$ related to overshoot.

The above does not mean that LMRDs have no practical value. We need to extend the comparison. We may introduce into the picture the time or space. Using the time, we may consider how the loop performance changes over time. We have to be aware that a plant is not immutable or constant. It varies all the time, due to the products used and their changing properties, variations in production demands, atmospheric fluctuations, the wear and tear of the installation components, plant failures, and human impacts. But the control loop often remains unmodified, and therefore one would like to know how the control performance accommodates to these changes. We would like to make the control loop robust enough to not lose performance. This effect is known in engineering practice as controller sustainability.

The extension in space means the comparison between various loops in complex multi-loop systems. Such a task is called loop benchmarking or homogeneity analysis, as we would wish to have all the loops operating similarly, because the ones which behave in a different way (so-called discordantly) may cause the whole system to deteriorate in performance. These aspects have already been introduced and analyzed [45].

4. Industrial Validation

We used data from the ammonia production installation located at Grupa Azoty Zakłady Azotowe “Puławy” SA in Poland. The production utilizes technology of the autothermal reforming of methane CH_4 with the utilization of oxygen: pure and in the form of processed air [45]. Figure 19 presents a schematic diagram of the considered ammonia production plant.

The plant is equipped with a modern control system that uses a hierarchical advanced process control strategy with a basic layer utilizing PID control algorithms, which are supervised using model predictive control [46]. All PID loops are well-tuned and maintained. The supervisory dynamic optimization allows optimal system operation.

As the data selection was crucial for the subsequent analysis, much attention was given to using comparable and credible time series from normal operating regimes. We used a dataset from 14 consecutive months (July 2020–August 2021), satisfying a 1 min sampling time. To allow data comparability assumptions, it was ensured that the natural gas consumption within these periods varied at most $\pm 1.5\%$. The load was constant and its fluctuations were process related. Time series were taken from the plant information system. The dataset comprised control error records from 22 PID loops: 12 flow, 2 level, 1 pressure, and 7 temperature controls. Detailed information about these loops is limited by the Grupa Azoty security regulations.

Such construction of data files, i.e., 22 loops collected in 14 months, allowed two analytical perspectives. First, we could compare the homogeneity between the loops. Therefore, we used a single month (July 2020) and plot LMRDs for 22 loops. Two LMRDs

were plot. Figure 20 shows the L-skewness versus L-Cv LMRD(τ_2, τ_3) diagram, while a L-kurtosis versus L-skewness LMRD(τ_3, τ_4) plot is sketched in Figure 21.

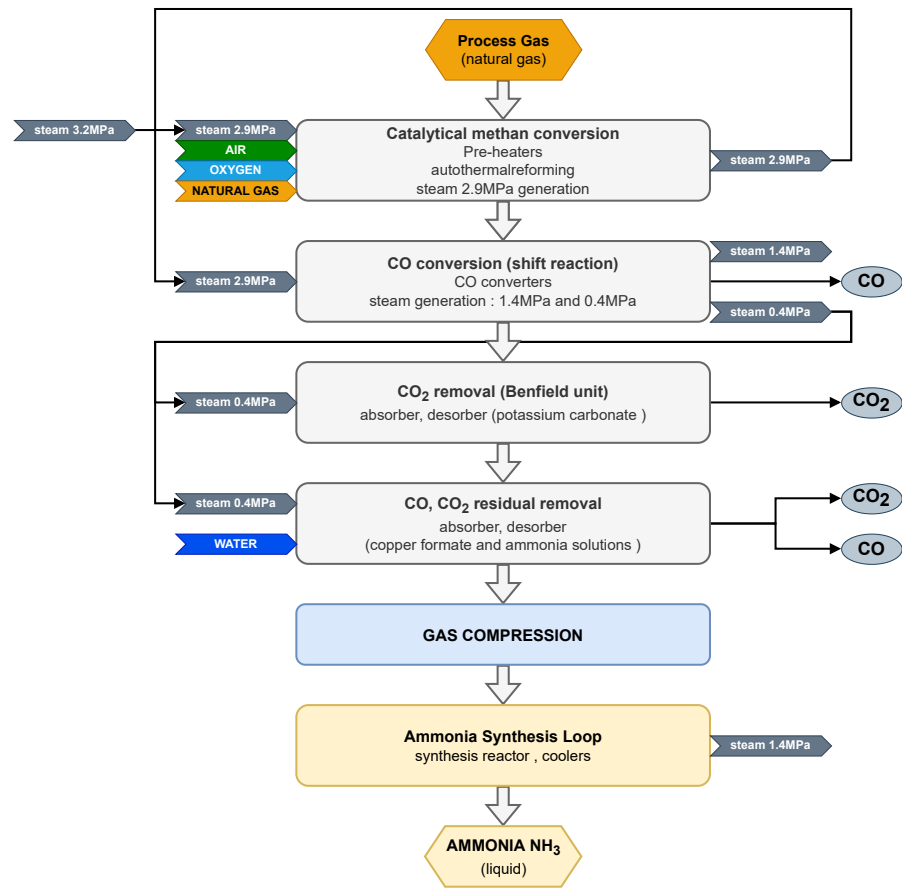


Figure 19. Schematic diagram of the ammonia production plant.

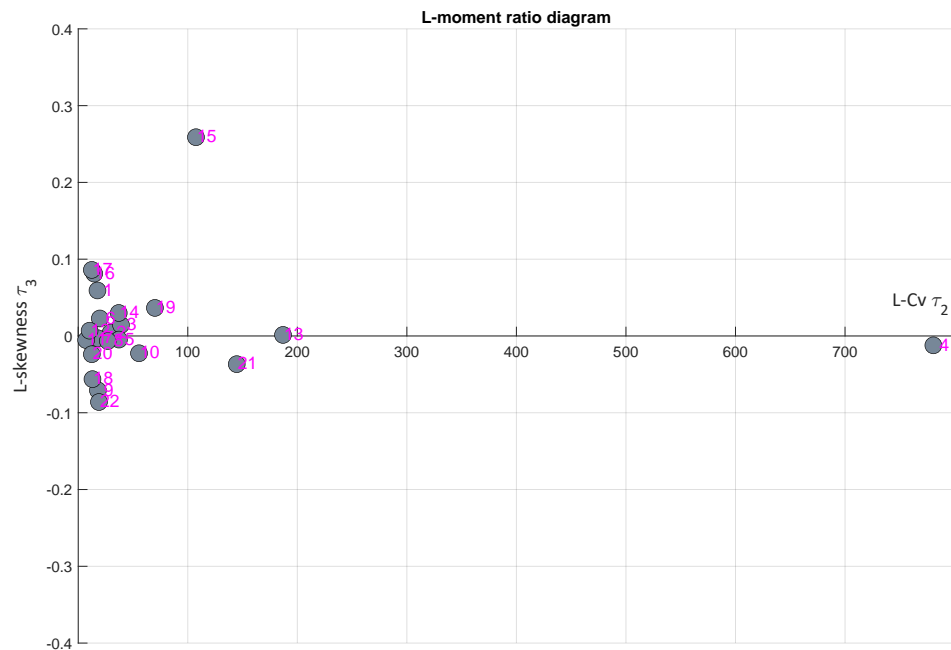


Figure 20. The LMRD(LcV, τ_3) for July 2020.

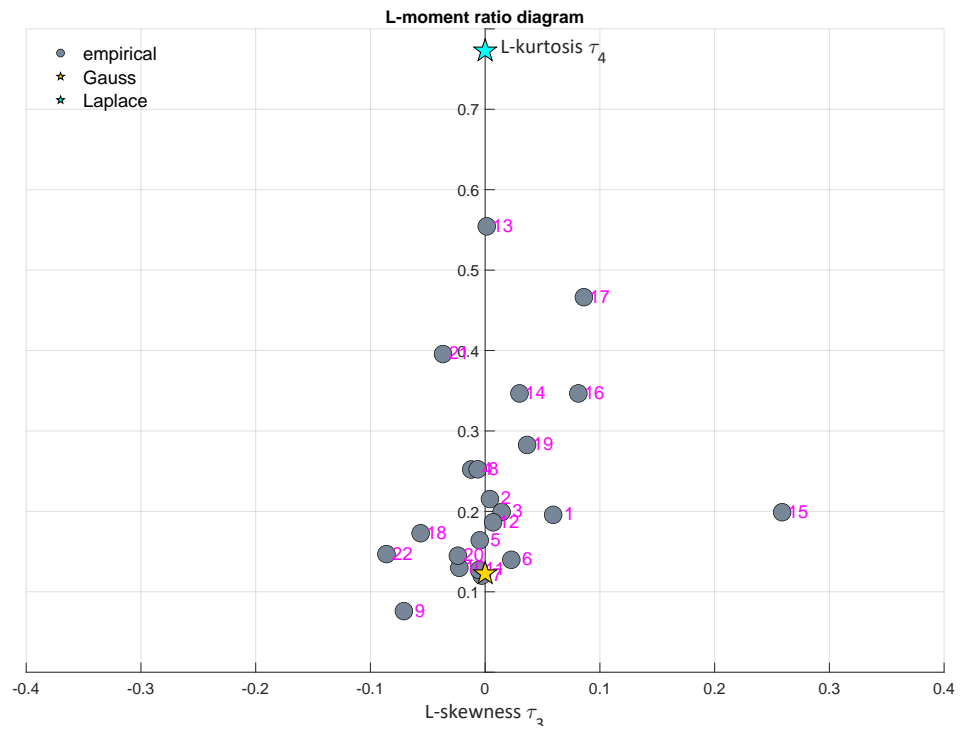


Figure 21. The LMRD(τ_3, τ_4) for July 2020.

The second perspective, i.e., a single loop #15 but a showing a comparison on a monthly basis is presented in the next plots. Figure 22 presents the LMRD(τ_2, τ_3) and Figure 23 the LMRD(τ_3, τ_4) plot.

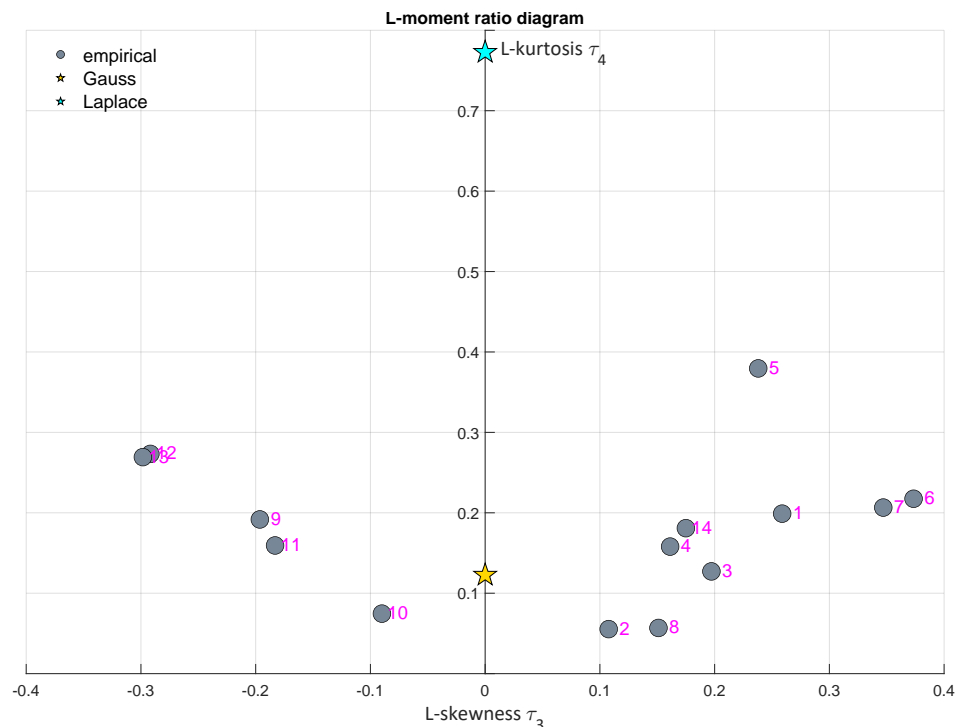


Figure 22. The LMRD(LcV, τ_3) for loop #15.

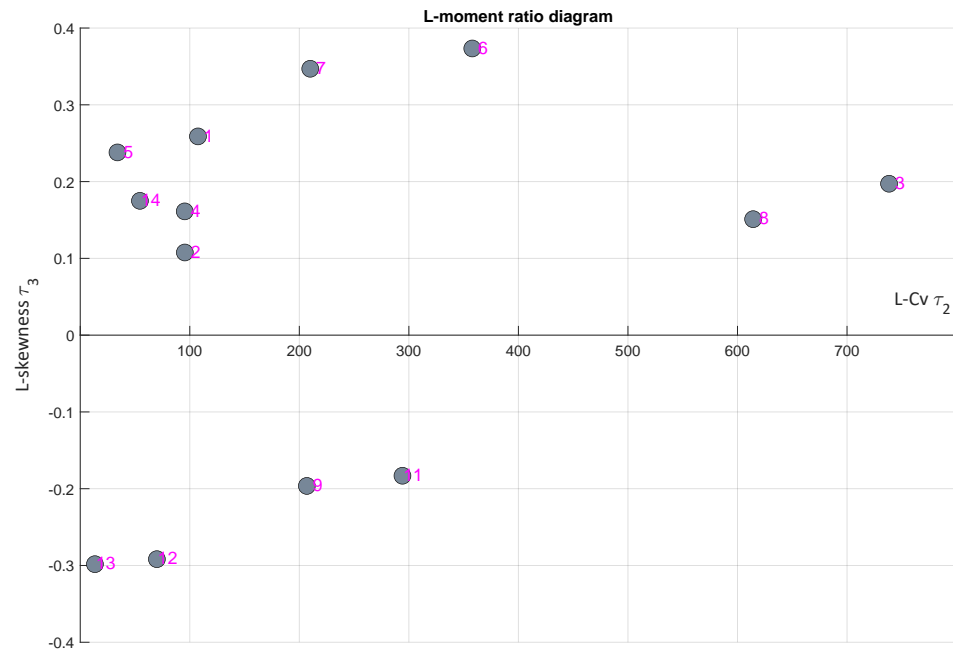


Figure 23. The LMRD(τ_3, τ_4) for loop #15.

A review of the above plots allows making observations. First, all the loops worked properly and they were well-tuned, as the LMRD(LcV, τ_3) and LMRD(τ_3, τ_4) show a concentration of points around L-skewness equal to zero. Loop #15, which was selected for the time perspective, seems to be the most challenging. This observation is confirmed with two other diagrams, which show large variations, which were most probably related to process nonlinearities.

Industrial validation justified the applicability of LMRDs in practice. In this project, they were used to confirm the positive results of the control system rehabilitation, which were associated with the comprehensive tuning activities and the implementation of the APC system. Simulations allowed combining the loop control performance with the point location in the diagram. As a consequence, this knowledge allowed the interpretation of the industrial data.

5. Conclusions and Further Research

The main contribution of this paper is the introduction of L-moment ratio diagrams into control engineering research and practice. Though they constitute a well-established methodology in the life sciences, they remain unknown in control engineering. However, their properties are very promising and might bring new perspective to the engineering context. We also introduced a new LMRD(l_2, τ_4) that better fits the CPA task.

The simulation analysis showed the feasibility of the proposed approach. Simulations allowed assess to and comparison of various theoretical scenarios, which enabled generalizing the observations. It was shown that a proper combination of the diagrams allowed determining poor and good tuning. We demonstrated that one plot, whichever we used, was not enough. However, the combination of two diagrams, LMRD(τ_2, τ_3) and the LMRD(l_2, τ_4) or LMRD(τ_3, τ_4) helped. The idea of using the LMRDs in control engineering is novel, because the L-moments common in extreme analysis remain unknown in control engineering. This works shows that the idea of moment ratio plots can be useful, because a given loop can be described by a single point, whose location on the LMRD plot describes certain loop properties. Moreover, in the case of more loops or data from different time periods, we obtained an tool that allows their easy comparison.

Simulations give some theoretical hints that should be cross validated in practice. Validation of the proposed technology was conducted using long-term industrial data from a complex, multi-loop ammonia production plant. This demonstrated several facts. First

of all, direct use of the LMRDs was not so meaningful, as we obtained a single point in the two-dimensional plane that did not allow drawing decisive conclusions. However, there was nothing to prevent expanding the research perspective. The introduction of time into the analysis allowed observing and measuring loop performance fluctuations in time—control sustainability. Benchmarking between numerous loops operating in a single, but complex multi-loop system, allowed benchmarking them, to measure their homogeneity and to detect the loops that stood apart from the rest. Such single outlying loops might form performance bottlenecks, and their tuning might seriously improve the overall system performance.

This paper showed that still there is much to be done in this research area, especially in combining simulations with engineering practice. Further research should address two areas. Theoretical investigations would help to analyze the LMRD plots themselves, in order to label certain points or sectors in the LMRD plots as responsible for certain loop behaviors. Further and extensive industrial validation would allow embedding practical effects into the LMRD. In particular, observation of the loop time paths in an LMRD diagram might be useful in loop (system) diagnosis and maintenance.

Author Contributions: Conceptualization, P.D.D.; methodology, P.D.D.; software, P.D.D.; validation, K.D. and R.G.; investigation, P.D.D. and R.G.; data curation, P.D.D. and R.G.; writing—original draft preparation, P.D.D.; writing—review and editing, K.D. and R.G.; visualization, P.D.D. and R.G.; supervision, K.D.; project administration, K.D.; funding acquisition, K.D. All authors have read and agreed to the published version of the manuscript.

Funding: This research was funded by Polish National Centre for Research and Development grant number POIR.01.02.00-00-0041/16.

Institutional Review Board Statement: Not applicable.

Informed Consent Statement: Not applicable.

Data Availability Statement: The data presented in this study are available on request from the corresponding author.

Conflicts of Interest: The authors declare no conflicts of interest.

Abbreviations

The following abbreviations are used in this manuscript:

κ	overshoot
T_{set}	settling time
APC	Advanced Process Control
CPA	Control Performance Assessment
CV	Controlled Variable
EVA	Extreme Value Analysis
GEV	Generalized Extreme Value
IAE	integral absolute error
ISE	integral square error
ITAE	Integral of Time-weighted Absolute Error
K4P	Four Parameters Kappa distribution
KPI	Key Performance Indicator
LMRD	L-Moment Ratio Diagram
MAD	Mean Absolute Deviation
MRD	Moment Ratio Diagram
PDF	Probability Density Function
PID	Proportional-Integrating-Derivative
PV	Process Variable
STP	setpoint

References

1. Jelali, M. *Control Performance Management in Industrial Automation: Assessment, Diagnosis and Improvement of Control Loop Performance*; Springer: London, UK, 2013.
2. Ordys, A.; Uduehi, D.; Johnson, M.A. *Process Control Performance Assessment—From Theory to Implementation*; Springer: London, UK, 2007.
3. Gomez, D.; Moya, E.J.; Baeyens, E. Control Performance Assessment: A General Survey. In *Distributed Computing and Artificial Intelligence. Advances in Intelligent and Soft Computing*; de Leon F. de Carvalho, A.P., Rodríguez-González, S., De Paz Santana, J.F., Rodríguez, J.M.C., Eds.; Springer: Berlin/Heidelberg, Germany, 2010; Volume 79.
4. O'Neill, Z.; Li, Y.; Williams, K. HVAC control loop performance assessment: A critical review (1587-RP). *Sci. Technol. Built Environ.* **2017**, *23*, 619–636. [[CrossRef](#)]
5. Huba, M. Performance Measures and the Robust and Optimal Control Design. *IFAC-PapersOnLine* **2018**, *51*, 960–965. [[CrossRef](#)]
6. Starr, K.D.; Petersen, H.; Bauer, M. Control loop performance monitoring—ABB's experience over two decades. *IFAC-PapersOnLine* **2016**, *49*, 526–532. [[CrossRef](#)]
7. Bauer, M.; Horch, A.; Xie, L.; Jelali, M.; Thornhill, N. The current state of control loop performance monitoring—A survey of application in industry. *J. Process Control* **2016**, *38*, 1–10. [[CrossRef](#)]
8. Knospe, C. PID control. *IEEE Control Syst. Mag.* **2006**, *26*, 30–31. [[CrossRef](#)]
9. Åström, K.J.; Murray, R. *Feedback Systems: An Introduction for Scientists and Engineers*; Princeton University Press: Princeton, NJ, USA; Oxford, UK, 2012.
10. Samad, T. A Survey on Industry Impact and Challenges Thereof [Technical Activities]. *IEEE Control Syst. Mag.* **2017**, *37*, 17–18.
11. Åström, K.J. Computer control of a paper machine—An application of linear stochastic control theory. *IBM J.* **1967**, *11*, 389–405. [[CrossRef](#)]
12. Domański, P.D. *Control Performance Assessment: Theoretical Analyses and Industrial Practice*; Springer International Publishing: Cham, Switzerland, 2020.
13. Gao, X.; Yang, F.; Shang, C.; Huang, D. A review of control loop monitoring and diagnosis: Prospects of controller maintenance in big data era. *Chin. J. Chem. Eng.* **2016**, *24*, 952–962. [[CrossRef](#)]
14. Spinner, T.; Srinivasan, B.; Rengaswamy, R. Data-based automated diagnosis and iterative retuning of proportional-integral (PI) controllers. *Control Eng. Pract.* **2014**, *29*, 23–41. [[CrossRef](#)]
15. Bialic, G.; Blachuta, M.J. Performance Assessment of Control Loops with PID controllers Based on Correlation and Spectral Analysis. In Proceedings of the 12th IEEE International Conference on Methods and Models in Automation and Robotics, MMAR'2006, Ann Arbor, MI, USA, 10–12 July 2006.
16. Harris, T.J.; Yu, W. Controller assessment for a class of non-linear systems. *J. Process Control* **2007**, *17*, 607–619. [[CrossRef](#)]
17. Veronesi, M.; Visioli, A. Performance Assessment and Retuning of PID Controllers for Load Disturbance Rejection. *IFAC Proc. Vol.* **2012**, *45*, 530–535. [[CrossRef](#)]
18. Srinivasan, B.; Spinner, T.; Rengaswamy, R. Control loop performance assessment using detrended fluctuation analysis (DFA). *Automatica* **2012**, *48*, 1359–1363. [[CrossRef](#)]
19. Knierim-Dietz, N.; Hanel, L.; Lehner, J. *Definition and Verification of the Control Loop Performance for Different Power Plant Types*; Technical Report; Institute of Combustion and Power Plant Technology, University of Stuttgart: Stuttgart, Germany, 2012.
20. Afshar Khamseh, S.; Khaki Sedigh, A.; Moshiri, B.; Fatehi, A. Control performance assessment based on sensor fusion techniques. *Control Eng. Pract.* **2016**, *49*, 14–28. [[CrossRef](#)]
21. Chaber, P.; Domański, P.D. Control Assessment with Moment Ratio Diagrams. In *Advanced, Contemporary Control*; Pawelczyk, M., Bismor, D., Ogonowski, S., Kacprzyk, J., Eds.; Springer Nature: Cham, Switzerland, 2023; pp. 530–535.
22. Craig, C.C. A New Exposition and Chart for the Pearson System of Frequency Curves. *Ann. Math. Stat.* **1936**, *7*, 16–28. [[CrossRef](#)]
23. Bobee, B.; Perreault, L.; Ashkar, F. Two kinds of moment ratio diagrams and their applications in hydrology. *Stoch. Hydrol. Hydraul.* **1993**, *7*, 41–65. [[CrossRef](#)]
24. Hosking, J.R.M. L-Moments: Analysis and Estimation of Distributions Using Linear Combinations of Order Statistics, *J. R. Stat. Soc. Ser. B* **1990**, *52*, 105–124. [[CrossRef](#)]
25. Lillo, C.; Leiva, V.; Nicolis, O.; Aykroyd, R.G. L-moments of the Birnbaum-Saunders distribution and its extreme value version: Estimation, goodness of fit and application to earthquake data. *J. Appl. Stat.* **2018**, *45*, 187–209. [[CrossRef](#)]
26. Giełczewski, M.; Piniewski, M.; Domański, P.D. Mixed statistical and data mining analysis of river flow and catchment properties at regional scale. *Stoch. Environ. Res. Risk Assess.* **2022**, *36*, 2861–2882. [[CrossRef](#)]
27. Podladchikova, O.; Lefebvre, B.; Krasnoselskikh, V.; Podladchikov, V. Classification of probability densities on the basis of Pearson's curves with application to coronal heating simulations. *Nonlinear Process. Geophys.* **2003**, *10*, 323–333. [[CrossRef](#)]
28. Fawad, M.; Ahmad, I.; Nadeem, F.A.; Yan, T.; Abbas, A. Estimation of wind speed using regional frequency analysis based on linear-moments. *Int. J. Climatol.* **2018**, *38*, 4431–4444. [[CrossRef](#)]
29. Louzada, F.; Ramos, P.; Perdoná, G. Different Estimation Procedures for the Parameters of the Extended Exponential Geometric Distribution for Medical Data. *Comput. Math. Methods Med.* **2016**, *2016*, 8727951. [[CrossRef](#)] [[PubMed](#)]
30. Valbuena, R.; Maltamo, M.; Mehtatalo, L.; Packalen, P. Key structural features of Boreal forests may be detected directly using L-moments from airborne lidar data. *Remote Sens. Environ.* **2017**, *194*, 437–446. [[CrossRef](#)]
31. Rousseeuw, P.J.; Leroy, A.M. *Robust Regression and Outlier Detection*; John Wiley & Sons, Inc.: New York, NY, USA, 1987.

32. Domański, P.D. Study on Statistical Outlier Detection and Labelling. *Int. J. Autom. Comput.* **2020**, *17*, 788–811. [[CrossRef](#)]
33. Ross, S.M. *Introduction to Probability and Statistics for Engineers and Scientists*, 5th ed.; Academic Press: London, UK, 2014.
34. Peel, M.; Wang, Q.; McMahon, T. The utility L-moment ratio diagrams for selecting a regional probability distribution. *Hydrol. Sci. J.* **2001**, *46*, 147–155. [[CrossRef](#)]
35. Hosking, J.R.M. Moments or L-Moments? An Example Comparing Two Measures of Distributional Shape. *Am. Stat.* **1992**, *46*, 186–189. [[CrossRef](#)]
36. Fischer, S.; Schumann, A. Robust flood statistics: Comparison of peak over threshold approaches based on monthly maxima and TL-moments. *Hydrol. Sci. J.* **2016**, *61*, 457–470. [[CrossRef](#)]
37. Zakaria, Z.A.; Shabri, A.; Ahmad, U.N. Estimation of generalized pareto distribution from censored flood samples using partial L-moments. *J. Math. Res.* **2011**, *3*, 112–120. [[CrossRef](#)]
38. Lee, S.H.; Maeng, S.J. Comparison and analysis of design floods by the change in the order of LH-moment methods. *Irrigation and Drainage. J. Int. Comm. Irrig. Drain.* **2003**, *52*, 231–245. [[CrossRef](#)]
39. Wan Zin, W.Z.; Jemain, A.A.; Ibrahim, K. The best fitting distribution of annual maximum rainfall in Peninsular Malaysia based on methods of L-moment and LQ-moment. *Theor. Appl. Climatol.* **2009**, *96*, 337–344. [[CrossRef](#)]
40. Wang Q.J. Estimation of the GEV distribution from censored samples by method of partial probability weighted moments. *J. Hydrol.* **1990**, *120*, 103–110. [[CrossRef](#)]
41. Vargo, E.; Pasupathy, R.; Leemis, L. Moment-Ratio Diagrams for Univariate Distributions. *J. Qual. Technol.* **2010**, *42*, 1–11. [[CrossRef](#)]
42. Åström, K.J.; Hägglund, T. Benchmark Systems for PID Control. *IFAC Proc. Vol.* **2000**, *33*, 165–166. [[CrossRef](#)]
43. Borak, S.; Härdle, W.; Weron, R. *Stable Distributions*; SFB 649 Discussion Paper 2005-008; Humboldt-Universität zu Berlin: Berlin, Germany, 2005.
44. Åström, K.J.; Hägglund, T. New tuning methods for PID controllers. In Proceedings of the 3rd European Control Conference, Roma, Italy, 5–8 September 1995; pp. 2456–2462.
45. Domański, P. D.; Jankowski, R.; Dziuba, K.; Góra, R. Assessing Control Sustainability Using L-Moment Ratio Diagrams. *Electronics* **2023**, *12*, 2377. [[CrossRef](#)]
46. Dziuba, K.; Góra, R.; Domański, P.D.; Ławryńczuk, M. Multicriteria Ammonia Plant Assessment for the Advanced Process Control Implementation. *IEEE Access* **2020**, *8*, 207923–207937. [[CrossRef](#)]

Disclaimer/Publisher’s Note: The statements, opinions and data contained in all publications are solely those of the individual author(s) and contributor(s) and not of MDPI and/or the editor(s). MDPI and/or the editor(s) disclaim responsibility for any injury to people or property resulting from any ideas, methods, instructions or products referred to in the content.